

Fabrication and nanostructure of oriented FePt particles

Bo Bian^{a)} and David E. Laughlin

Data Storage Systems Center, Carnegie Mellon University, Pittsburgh, Pennsylvania 15213

Kazuhisa Sato and Yoshihiko Hirotsu

The Institute of Scientific and Industrial Research, Osaka University, Osaka 5670047, Japan

Thin films of oriented tetragonal FePt particles separated by amorphous alumina have been fabricated by electron beam evaporation. The ordering of the FePt particles without coarsening can be tailored by annealing conditions. The value of coercivity of the annealed film reached as high as 4.4 kOe. The perpendicular magnetic coercivity of the annealed film was slightly larger than in-plane coercivity. Some of the tetragonal FePt particles were found to have {111} twins and stacking faults. From our high-resolution electron microscopy observations, it was determined that central region of the ordered FePt particles tended to have *c*-axis perpendicular to the film plane.

© 2000 American Institute of Physics. [S0021-8979(00)46908-2]

I. INTRODUCTION

Areal density in longitudinal magnetic recording has been dramatically improved in recent years. Future higher magnetic storage density media with low noise is associated with a smaller magnetic grain size and a better magnetic isolation among the grains. For a given material, its maximum areal density will ultimately be limited by thermal stability.¹ To avoid thermal instability, materials with much higher magnetic anisotropy are needed for future magnetic recording media.²

The ordered equiatomic FePt phase with tetragonal $L1_0$ structure has high magnetocrystalline anisotropy, close to the 10^8 erg/cm³ regime, which is more than one order of magnitude larger than that of currently utilized hexagonal-close-packed (hcp) Co based alloys. The high magnetic anisotropy and good corrosion resistance make the $L1_0$ FePt compound an attractive material for magnetic recording media. Thin films of $L1_0$ FePt have been previously studied as possible magneto-optical media.^{3,4} Recently, Li and Lairson reported on magnetic recording on untextured FePt compound media prepared by magnetron sputtering on ZrO₂ disks with post-deposition annealing.⁵ These films exhibited very high magnetic coercivity, between 5 and 12 kOe. Weller *et al.* prepared films of (111) textured $L1_0$ FePt particles by electron beam coevaporation of Fe and Pt metal on SiN_x coated or thermally oxidized Si (001) substrates.⁶ Large coercivity of about 11 kOe was observed in a 12-nm-thick Fe₅₅Pt₄₅ film, indicating the presence of large anisotropy.

The magnetic hardness of small particles in the FePt alloy system generally depends on the structure, the size, the composition of the particles, and interaction between the particles. As the formation of $L1_0$ FePt particles usually requires adequate annealing to overcome the energy barrier for diffusion and superlattice ordering, concurrent grain coarsening during the ordering annealing process may occur if the particles are in close contact with each other. The grain coarsening and interaction among the particles will have im-

portant effects on magnetic properties. It has been reported that physical gaps of 2–5 nm appear to be sufficient to decouple the magnetic grains.⁷ In order to have a better understanding of the relationship between magnetic properties and microstructure of small FePt particles, we have prepared films with desired nanostructures. It is advantageous to have films of FePt particles separated by physical gaps, which can prevent grain coarsening during annealing and eliminate interaction between the particles. In this article, we report on a new method to prepare films of oriented $L1_0$ FePt particles separated by amorphous (*a*-)Al₂O₃. We will also present the nanostructure of the films as well as their magnetic properties.

II. EXPERIMENT

The sample preparation was performed in an electron-beam evaporation system with a base pressure of approximately 3×10^{-7} Pa. Pure Pt, Fe, and Al₂O₃ crystals were used as evaporation sources. Freshly cleaved NaCl (100) crystals, and clean polished (100) MgO wafers were used as substrates. The substrates were kept at approximately 400 °C during the deposition. First, Pt was deposited at 0.1 nm/min onto the substrate. Then, Fe was deposited at 0.4 nm/min onto the substrate with the Pt. A continuous cover layer of *a*-Al₂O₃ with a thickness greater than 5 nm was deposited further without breaking vacuum. The average thicknesses of all the Pt and Fe layers were set to be 1.5 and 1.0 nm, respectively. To also obtain a film with only Pt particles, a part of the NaCl substrates was shielded from the Fe flux after the Pt deposition. Postannealing of the *a*-Al₂O₃/Fe/Pt films on the NaCl and MgO substrates was done at 600 °C for different time intervals in a vacuum better than 2×10^{-5} Pa. The NaCl substrates were immersed into distilled water to remove the *a*-Al₂O₃/Pt or *a*-Al₂O₃/Fe/Pt films, and the films were mounted on copper microgrids for transmission electron microscopy (TEM) observations at 200 and 300 kV. In-plane and perpendicular magnetization hysteresis loops of the as-deposited and annealed films on NaCl or MgO substrates were generally measured at room temperature with a superconducting quantum interference device

^{a)}Electronic mail: bobian@ece.cmu.edu

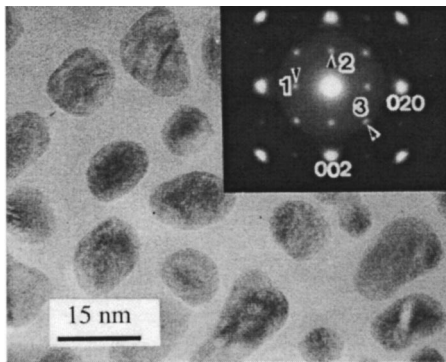


FIG. 1. TEM image and corresponding SAED pattern of the $a\text{-Al}_2\text{O}_3/\text{Fe}/\text{Pt}$ film annealed at 600°C for 6 h. Dispersed FePt particles are visible. In the SAED pattern, there are $\{001\}$ and $\{110\}$ superlattice reflections due to $L1_0$, together with the $\{002\}$ fundamental reflections.

magnetometer (SQUID). During the measurements the magnetic field was parallel to the $\langle 100 \rangle$ direction of the substrates.

III. RESULTS AND DISCUSSION

TEM observations of as-deposited $a\text{-Al}_2\text{O}_3/\text{Pt}$ and $a\text{-Al}_2\text{O}_3/\text{Fe}/\text{Pt}$ films showed that Pt crystals exhibited a well-defined morphology with facets whereas FePt particles appeared to be somewhat island-like. As the number density of the FePt particles was close to that of Pt particles, we assume that Pt particles acted as seed particles for the growth of Fe crystallites. From selected area electron diffraction (SAED) patterns, it was known that the Pt crystals were $\langle 100 \rangle$ oriented and the Fe crystallites had a body-centered-cubic (bcc) structure. The Fe crystallites were not polycrystalline but fiber textured in the $\langle 100 \rangle$ and $\langle 110 \rangle$ directions.⁸

Figure 1 shows TEM image and corresponding SAED pattern of the $a\text{-Al}_2\text{O}_3/\text{Fe}/\text{Pt}$ film annealed at 600°C for 6 h. The FePt particles are dispersed. The average size of the particles in this film is estimated to be 12 nm. The average space between particles is approximately 4 nm. In the SAED pattern, besides the $\{002\}$ fundamental reflections, $\{001\}$ and $\{110\}$ superlattice reflections due to $L1_0$ are visible, implying the coexistence of three-variant ordered domains of the tetragonal phase in the film. This result was confirmed by nanobeam electron diffraction (NBD) examination by focusing an electron nanoprobe on local regions of ordered FePt particles. Any one of the three $\langle 100 \rangle$ axes of the face-centered-cubic (fcc) Pt parent phase can correspond to the tetragonal c axis of the superstructure. From the NBD patterns of $a\text{-Al}_2\text{O}_3/\text{Fe}/\text{Pt}$ films annealed at 600°C for different time intervals, it was found that c/a ratio decreased as annealing progressed. The c/a ratio for $a\text{-Al}_2\text{O}_3/\text{Fe}/\text{Pt}$ film annealed at 600°C for 12 h is approximately 0.97, indicating a ordered state.

Figure 2 shows SAED pattern of a 600°C annealed $a\text{-Al}_2\text{O}_3/\text{Fe}/\text{Pt}$ film obtained with the electron beam parallel to the $\langle 110 \rangle$ direction of the film. The 110 and 100 superlattice reflections due to $L1_0$ and the 111, 200 fundamental reflections are observed. It should be noted that in the SAED pattern there are extra reflections as marked by arrows. The

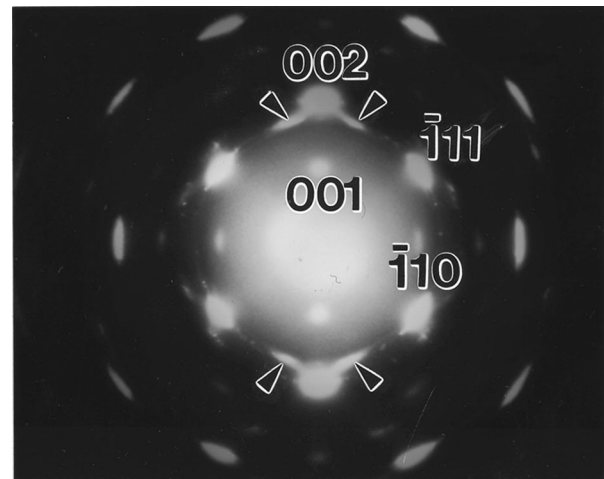


FIG. 2. SAED pattern of 600°C annealed $a\text{-Al}_2\text{O}_3/\text{Fe}/\text{Pt}$ film obtained with the electron beam parallel to the $\langle 110 \rangle$ direction of the film. Besides the superlattice reflections due to $L1_0$ and the fundamental reflections, there exist extra reflections (as marked by arrows) from $\{111\}$ twins and stacking faults.

extra reflections can be indexed as reflections from $\{111\}$ twins and stacking faults. It has been reported that $\{111\}$ twins but not $\{110\}$ twins were observed in single crystalline FePt films.⁹ From our dark image observation by applying 111 reflections, the existence of $\{111\}$ twins and stacking faults in some FePt particles was confirmed.

Figure 3 shows in-plane hysteresis loops for $a\text{-Al}_2\text{O}_3/\text{Fe}/\text{Pt}$ films on the (100) MgO substrate (unannealed and annealed at 600°C for different times). The as-deposited $a\text{-Al}_2\text{O}_3/\text{Fe}/\text{Pt}$ film is magnetically soft. The coercivities of the films increase dramatically upon annealing at 600°C , implying the formation of hard magnetic FePt phase. As annealing time increases, the coercivity increases but the magnetic squareness decreases. Our magnetic measurements showed that the magnetic properties of all the $a\text{-Al}_2\text{O}_3/\text{Fe}/\text{Pt}$ films on both NaCl and MgO (100) substrates were similar. The coercivities of the 600°C , 6 h annealed $a\text{-Al}_2\text{O}_3/\text{Fe}/\text{Pt}$ films on (100) NaCl and MgO substrates were 3.5 and 3.3 kOe, respectively. From the similarity of the magnetic data of the films on both substrates, we are inclined to believe that similar microstructure change, upon annealing, occurred for the $a\text{-Al}_2\text{O}_3/\text{Fe}/\text{Pt}$ films on both substrates.

The annealed $a\text{-Al}_2\text{O}_3/\text{Fe}/\text{Pt}$ films on both the substrates had higher perpendicular coercivities as compared with in-

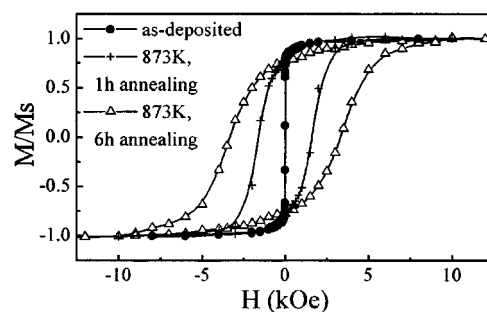


FIG. 3. In-plane hysteresis loops for $a\text{-Al}_2\text{O}_3/\text{Fe}/\text{Pt}$ films on the (100) MgO substrate (unannealed and annealed at 600°C for different times).

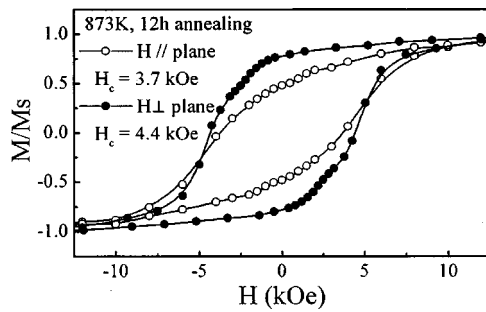


FIG. 4. In-plane and perpendicular magnetization hysteresis loops of the $a\text{-Al}_2\text{O}_3/\text{Fe}/\text{Pt}$ film on the MgO (100) substrate (annealed at 600°C for 12 h).

plane coercivities. Figure 4 shows in-plane and perpendicular magnetization hysteresis loops of the $a\text{-Al}_2\text{O}_3/\text{Fe}/\text{Pt}$ film on the MgO (100) substrate (annealed at 600°C for 12 h). The obtained perpendicular coercivity is about 4.4 kOe, which is larger than that of in-plane coercivity of 3.7 kOe. In order to understand the origin of the difference between in-plane and perpendicular magnetization loops of the annealed films, high-resolution electron microscopy (HREM) observation of the $a\text{-Al}_2\text{O}_3/\text{Fe}/\text{Pt}$ films annealed at 600°C was undertaken. Figure 5 shows a HREM image of a typical ordered FePt particle. The particle exhibits several structural domains corresponding to the three variants of the tetragonal structure. The c axis of the central region of the particle is perpendicular to the film plane and that of the other two orthogonal variants in the outer regions of the crystallite, are in the horizontal plane. The easy axis of magnetization of the $L1_0$ structure is along its c axis. The difference between perpendicular and in-plane coercivities might arise from the

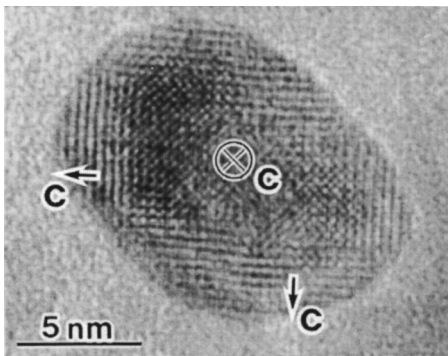


FIG. 5. HREM image of a typical ordered FePt particle. The c axis of the central region of the particle is perpendicular to the film plane and that of the other two orthogonal variants in the outer regions of the crystallite, are in the horizontal plane.

fact that the central regions with c axis perpendicular to the film plane occupy a larger proportion of the whole volume of the particles.

The present $L1_0$ FePt particles can be regarded as single magnetic domain particles without exchange interaction due to their small size and well-separated nature. For a random distribution of FePt single domain particles with uniaxial anisotropy, coercivity $H_c \sim 58$ kOe can be expected ($H_c \sim K/M_s$ assuming uniaxial anisotropy $K \sim 6.6 \times 10^7$ erg/cm³ and saturation magnetization $M_s \sim 1140$ emu/cm³).¹⁰ The value of the maximum coercivity obtained in the present oriented FePt particles is much less than the expected value for polycrystalline FePt particles. The comparably lower values of the coercivities are possibly due to degree of ordering and thermal effects as the particle size is very small. In order to estimate the influence of thermal effect, we measured coercivities of the FePt particles at 10 K. The result showed that the coercivities of the particles at 10 K is less than double of the coercivities measured at room temperature. It has been reported that the density of $\{111\}$ twins influences the magnetic properties of single crystalline $L1_0$ FePt films.⁹ The $\{111\}$ twins and stacking faults, and boundaries of three variant of crystalline domains in the present FePt particles might have significant effect on the hard magnetic properties of the FePt films.

IV. CONCLUSION

We have prepared films of oriented $L1_0$ FePt particles separated by $a\text{-Al}_2\text{O}_3$. The coercivities of the FePt particles can be tailored by annealing conditions. The isolated FePt particles shows little coarsening during annealing. Some of the tetragonal FePt particles are found to have (111) twins and stacking faults. The perpendicular magnetic coercivity of the annealed films is slightly larger than in-plane coercivity. From our high-resolution electron microscopy observation, it is found that c axis of the central region of the particles tends to have c axis perpendicular to the film plane.

¹E. S. Murdock, R. F. Simmons, and R. Davidson, *IEEE Trans. Magn.* **28**, 3078 (1992).

²D. N. Lambeth, E. M. T. Velu, G. H. Bellesis, L. L. Lee, and D. E. Laughlin, *J. Appl. Phys.* **79**, 4496 (1996).

³B. M. Lairson, M. R. Visokay, R. Sinclair, and B. M. Clemens, *Appl. Phys. Lett.* **62**, 639 (1993).

⁴R. F. C. Farrow, D. Weller, R. F. Marks, M. F. Toney, A. Cebollada, and G. R. Harp, *J. Appl. Phys.* **79**, 5967 (1996).

⁵N. Li and B. M. Lairson, *IEEE Trans. Magn.* **35**, 1077 (1999).

⁶D. Weller, A. Moser, L. Folks, M. E. Best, W. Lee, M. F. Toney, M. Schwickert, J.-U. Thiele, and M. F. Doerner, presented at TMRC, San Diego, 1999 (unpublished).

⁷T. Yogi and T. A. Nyuyen, *IEEE Trans. Magn.* **29**, 307 (1993).

⁸Bo Bian, K. Sato, Y. Hirotsu, and A. Makino, *Appl. Phys. Lett.* **75**, 3686 (1999).

⁹M. H. Hong, K. Hono, and M. Watanabe, *J. Appl. Phys.* **84**, 4403 (1998).

¹⁰S. Stavroyiannis, I. Pangiotopoulos, D. Niarchos, J. A. Christodoulides, Y. Zhang, and G. C. Hadjipanayis, *Appl. Phys. Lett.* **73**, 3453 (1998).